Available online at www.sciencedirect.com
SCIENCE DIRECT®
Surface Science 595 (2005) 183–193
SURFACE SCIENCE
www.elsevier.com/locate/susc

The atomic surface structure of $SrTiO_3(001)$ in air studied with synchrotron X-rays

V. Vonk [a,b,*], S. Konings [a], G.J. van Hummel [b], S. Harkema [b], H. Graafsma [a]

[a] *European Synchrotron Radiation Facility, 6 rue Jules Horowitz, 38043 Grenoble, France*
[b] *Low Temperature Division and MESA + Research Institute, Faculty of Science and Technology, University of Twente, P.O. Box 217, 7500 AE Enschede, The Netherlands*

Received 25 April 2005; accepted for publication 14 August 2005
Available online 31 August 2005

Abstract

The atomic surface structure of single terminated $SrTiO_3(001)$ (1×1) is investigated employing surface X-ray diffraction. In order to obtain these surfaces a special treatment is needed consisting of chemical etching and annealing. Since this is done in an aqueous and subsequently oxygen environment, after which the crystals are kept at ambient conditions, the surface is studied in air. Crystal truncation rods are measured and several models that are proposed in literature in recent years are tested against the experimental data. These models include surface rumpling, low temperature-like distortions, strontium adatom and lateral displacement distortions for both TiO_2 and SrO-terminated surfaces. None of these models represents the data very accurately. A much better fit to the experimental results is obtained by using a model in which a TiO_2-terminated crystal is covered by an oxygen layer.

Keywords: SXRD; Complex oxides; Surface relaxation and reconstruction; Surfaces in ambient environment

1. Introduction

Strontium–titanate, $SrTiO_3$ (STO), falls within the class of perovskite-type oxides, having general formula ABO_3. The A- and B-sites can be occupied by elements with different valencies and different ionic radii and the properties and structures of these materials are closely related to the size of the cations and anions. Most of the perovskites show a transition from cubic to tetragonal, and with that a change in properties, upon cooling through a critical temperature [1]. Although $SrTiO_3$ undergoes a structural phase transition around 110 K, similar to $BaTiO_3$, it is not ferro-electric in the

* Corresponding author. Address: Low Temperature Division and MESA + Research Institute, Faculty of Science and Technology, University of Twente, P.O. Box 217, 7500 AE Enschede, The Netherlands.
E-mail address: v.vonk@tnw.utwente.nl (V. Vonk).
URL: http://lt.tnw.utwente.nl (V. Vonk).

0039-6028/$ - see front matter © 2005 Elsevier B.V. All rights reserved.
doi:10.1016/j.susc.2005.08.010

tetragonal phase [2]. This has lead to a series of publications on the structure and properties of bulk $SrTiO_3$ [3–7].

Recently, $SrTiO_3$ has gained interest in the micro-electronics industry, because of the need for materials which have small leak-currents. Furthermore, STO is used on a large scale as substrate material for the growth of thin film perovskite-type materials, like high-T_c superconductors. In this case the substrate surface structure and its control are of great interest [8].

Different preparation methods and analysis techniques to elucidate the nature of the (0 0 1) surface have been employed over the past two decades, and at present single terminated surfaces can be obtained [9–11]. However, the atomic surface structure is still matter of debate. For example, it is well known, that depending on the annealing conditions different reconstructions occur [12–15]. Most studies agree that these reconstructions are formed by oxygen vacancies, while Kubo and Nozoye [16,17] propose a model in which an ordered Sr adatom occurs on the surface.

Here, we present the results of surface X-ray diffraction (SXRD) experiments carried out on two different single terminated crystals. Single termination is obtained by a special treatment consisting of chemical etching and annealing [11]. The etching process takes place in an aqueous environment and the anneal step in 1 bar of flowing oxygen after which the crystals are kept at ambient conditions before being used for thin film growth. By SXRD we intend to determine the surface structure of STO(0 0 1), its dependence on the preparation procedure and its stability in air. We tested different models presented in literature, but none of them is able to fit our experimental data. For this reason a new model is presented.

2. Atomic structure of $SrTiO_3$

2.1. $SrTiO_3$

The atomic structure of $SrTiO_3$, given in Fig. 1, can be seen as a network of sixfold oxygen co-ordinated titanium atoms, with strontium in the interstitial sites, leading to a stack of alternating TiO_2 and SrO layers. This means that the (0 0 1) face of a macroscopic crystal can have TiO_2 and/or SrO terminations. Bulk STO has space group $Pm\bar{3}m$, with $a = 3.901(1)$ Å [18] at room temperature, and all atoms occupy special positions with fractional co-ordinates as shown in Table 1.

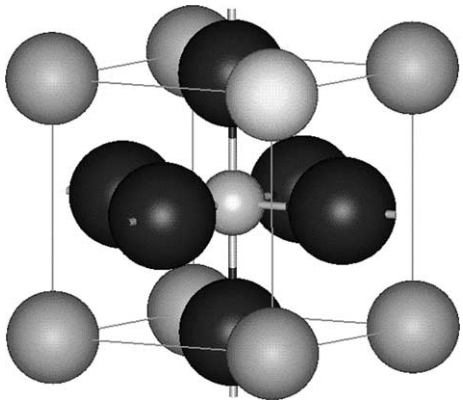

Fig. 1. The structure of bulk $SrTiO_3$. The largest atoms are oxygen, the smallest in the body-centre is titanium and strontium occupies the corners.

2.2. Shape of crystal truncation rods

Surface X-ray diffraction (SXRD) is a well-established technique to obtain structural information about crystal surfaces. It is based on the accurate determination of the intensity of the crystal truncation rods (CTRs), which are lines, in reciprocal space, parallel to the surface normal and interconnecting bulk Bragg peaks. The CTRs occur due to the termination of the crystal by its surface. A detailed description of the calculation of the CTR structure factors can be found elsewhere [19,20]. Usually the crystallographic directions are chosen

Table 1
Atomic fractional co-ordinates in bulk $SrTiO_3$

Atom	x	y	z
Sr	0	0	0
Ti	$\frac{1}{2}$	$\frac{1}{2}$	$\frac{1}{2}$
O1	$\frac{1}{2}$	$\frac{1}{2}$	0
O2	$\frac{1}{2}$	0	$\frac{1}{2}$
O3	0	$\frac{1}{2}$	$\frac{1}{2}$

such that h and k lay in the surface plane, while l is in the direction perpendicular to the surface. The CTRs are then measured along l.

Using the atomic positions from Table 1, the bulk contribution, or equivalently the scattering from bulk terminated STO, can be examined. It follows that the scattering contributions of O2 and O3 cancel each other when $(h + k)$ is odd. Furthermore, when disgarding the Debye–Waller parameter, crystal truncation rods (CTR's) exist with three different shapes. First, all CTRs for which $(h + k)$ is odd have identical shapes. Second, in the case of $(h + k)$ even, one can distinguish between CTRs with both h and k either even or odd.

3. Experimental

Optically polished z-cut crystals ($10 \times 10\ mm^2$) were obtained from Surfacenet GmbH (Rheine, Germany). The miscut angle, the angle between the optical surface normal and the crystallographic z-direction, is of the order of 0.1° or better. To obtain single termination, the as-received double terminated crystals are treated chemically in a NH_4F-buffered HF solution (BHF), with $4.5 < pH < 6.0$ [21]. It is believed that the SrO surface layers react to form a hydroxy-complex, which subsequently dissolves in water [22], thereby leaving a TiO_2-terminated surface. Finally, the surface is subjected to an annealing treatment at 950 °C in flowing oxygen for 2 h. Atomic force microscopy (AFM) measurements show that the terraces are 3.9 Å high, which corresponds to exactly one unit cell (3.901 Å), and that their ledges are particularly smooth. Furthermore, this surface treatment results in sharp (1×1) reflection high energy electron diffraction (RHEED) patterns [11], indicating that no reconstructions occur.

Two SXRD experiments were carried out at two different beamlines, ID03 [23] and BM26 [24], of the European Synchrotron Radiation Facility (ESRF). Two different samples were used, both prepared as described above. Both experiments were performed in air and at room temperature and resulted in the collection of several crystal truncation rods.

4. Results

The program ANA is used to integrate and correct the data, according to the particular diffraction geometry as described elsewhere [25,26], in this way the measured data are reduced to structure factors. Symmetry equivalent structure factors are averaged and merged using the program AVE. Like in RHEED measurements, no fractional order peaks are found for both samples, indicating that no planar reconstruction occurs. The validity of this finding will be discussed in more detail further on. This means that for both samples the planar space group P4mm is used in the merging procedure, which also gives a reasonable agreement factor. An overview of the results for the two samples is given in Table 2.

Although the data set of crystal 1 contains more reflections and crystal truncation rods than that of crystal 2, the overall multiplicity is close to one, meaning that of the set of eight symmetry equivalent reflections only one is measured. The resulting estimated standard deviations (e.s.d.'s), which are then only based on photon-counting statistics, are less realistic than those of the data set of crystal 2. The agreement factor, R_{merge}, of 6.1% for the data set of crystal 2 is an indication that the systematic errors (e.g. alignment of the sample) are fairly small. The influence of the miscut angle on the positions of the reflections was not noticeable during data collection [27], therefore this effect

Table 2
Crystal data, experimental data and results of merging. In the last column the data sets of crystal 1 and 2 are merged by applying one scale factor between them

	Crystal 1	Crystal 2	Crystals 1 and 2
Termination	Single	Single	–
Miscut (deg)	–	0.07	–
Wavelength (Å)	0.725	0.778	–
Incident angle (deg)	0.25	1.0	–
No. measured points	231	262	493
No. unique points	197	122	217
No. CTRs	7	6	7
$\left(\frac{\sin(\theta)}{\lambda}\right)_{min}$	0.12	0.18	0.12
$\left(\frac{\sin(\theta)}{\lambda}\right)_{max}$	0.63	0.59	0.63
R_{merge} (%)[a]	8.2	6.1	10.7

[a] Agreement factor $R_{merge} = \frac{\sum_{hkl}\sum_i ||F_i(hkl)| - |F(hkl)||}{\sum_{hkl}\sum_i |F_i(hkl)|}$.

can be neglected. A further indication of the quality of the data can be obtained by merging both data sets, using a single scale factor between them. This assumes that the two samples are identical, as well as the experimental conditions, like temperature. The resulting agreement factor of 10.7% indicates the two data sets to be comparable, and of good quality. The two data sets are nevertheless dealt with independently in the remainder of this article, because that provides information about the reproducibility of the sample preparation.

5. Discussion

In the following sections four different literature models are discussed by testing them against our data. Although the preparation methods and experimental conditions can be quite different from ours, these models are used as a starting point for comparison with our data. The models include a variety of possible distortions that have been published to date. In order to minimize the number of fit parameters, the models have not been combined. In the end, the best fit is obtained by a new model, consisting of an oxygen overlayer on top of a TiO_2-terminated crystal.

The program ROD [28] is used to calculate structure factors and thus crystal truncation rods for a given model. ROD uses a χ^2-minimization method to determine the best fit parameters. As an indication of how well the model describes the measured data, the following commonly used parameter is calculated as well

$$R = \frac{\sum_{hkl} ||F_{\mathrm{obs}}(hkl)| - s|\ F_{\mathrm{calc}}(hkl)||}{\sum_{hkl} |F_{\mathrm{obs}}(hkl)|}. \qquad (1)$$

In case of the literature models, the proposed numerical values of the displacements are taken and only the overall scale factor s is fitted. In this way the shapes of the calculated CTRs are investigated and compared with the data. When possible, a fit procedure of the displacement and thermal parameters is run and those results are presented as well. However, not every literature model describes the data well enough to run a least squares fit procedure, because certain fit parameters get unrealistic values.

The following assumptions are made regarding the thermal parameters and surface roughness in the model. The atoms in the bulk have isotropic thermal parameters $B_{\mathrm{Sr}} = 0.62$ Å^2, $B_{\mathrm{Ti}} = 0.44$ Å^2 and $B_{\mathrm{O}} = 0.72$ Å^2, which are taken from Abramov et al. [18]. From the AFM measurements (Section 3) it is clear that on the terraces the surface is atomically flat. Furthermore, the miscut angle is small enough that it does not influence the positions of the CTRs (Section 4), and therefore the surface roughness is taken to be zero [27].

5.1. Rumpling of surface

Most of the theoretical [29–33] and experimental [34–37] studies carried out so far have assumed a model consisting of a bulk terminated surface, with slight rumpling and displacement of the topmost layers. Measurements and calculations have been performed for SrO, TiO_2 and mixed type of terminations. It is assumed that only displacements in the z-direction occur and that like in the case of rumpling for other ionic solids, the larger anions move towards the vacuum and the smaller cations towards the bulk. Although the displacements found with this model seem to be very reasonable, the studies do not agree with each other. Surprisingly enough in the TiO_2-terminated case, it seems that whereas the theoretical studies systematically find a relaxation towards the bulk of the outermost layer, the experiments systematically indicate the opposite.

The relaxations found by Bickel et al. [35], Cheng et al. [32] and Charlton et al. [37], are used to fit our experimental data. The resulting R-factors and χ^2-values are listed in the summary Table 4. In Fig. 2 the CTRs obtained by using the displacements found by Charlton et al. are plotted together with our data. For both TiO_2 and SrO as well as bulk termination three characteristic (see Section 2.2) CTRs are plotted. Clearly, the TiO_2-terminated model, which is close to bulk termination, describes the experimental data better than when using the SrO termination.

5.2. Low temperature-like structure

Bulk STO undergoes a cubic-to-tetragonal phase transition around 110 K [2]. The crystal

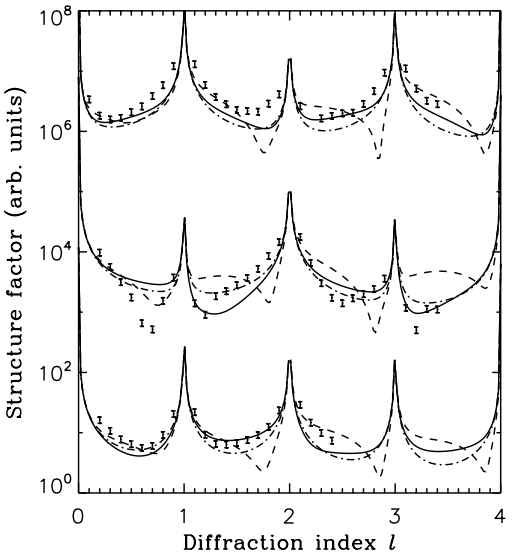

Fig. 2. Experimental data points and CTRs obtained with the relaxations for TiO_2 (solid) and SrO (dashed) terminations found by Charlton et al., as well as the bulk contribution (dash-dot). Shown are the 32 (top), 20 (middle) and 11 (bottom) CTRs, where the error bars indicate the experimental data points. The CTRs obtained with the SrO termination, have been scaled such that the overall scale factor is the same as for the TiO_2 and bulk termination.

structure changes from $Pm\bar{3}m$ to I4/mcm, by a rotation of the oxygen octahedra around one of the principle axes. The diagonals of the cubic structure are the principle axes of the tetragonal, low temperature, phase. Experimental evidence has been found for the existence of the low-temperature phase in the surface region at an onset temperature much higher than in the bulk. Mishina et al. [38] find a change in the (1 1 0) surface at a temperature around 150 K. They conclude that this is the low-temperature non-centrosymmetric phase due to the detection of optical second harmonics. Krainyukova and Butskii [39] conclude from their electron diffraction study, that at a temperature around 170 K the (0 0 1) surface transforms to the tetragonal phase.

Here, in the CTR calculations, we use this low-temperature model. It consists of a rotation of the oxygen around the fourfold titanium atom in the surface layer. Since by this rotation the planar space group changes from P4mm to P4, a domain-structure is assumed. Half of the surface consists of domains in which the oxygen rotate clockwise, while on the other half they rotate counter-clockwise within the domains. This distortion is, in first approximation, restricted to the topmost TiO_2 layer. Despite the absence of fractional order reflections, the validity of this model is tested, because the rotations are very small (typically 3°), and therefore the surface distorts only a little, which means that fractional order reflections are extremely weak. Due to the change in symmetry of the bulk, it is necessary to transform the diffraction indices, as well as the fractional co-ordinates from the cubic to the tetragonal structure [40]. To investigate only the effect of the oxygen concerned in the rotation on the CTRs, all other atoms are kept in their bulk positions and only the overall scale factor is refined. The resulting *R*-factors and χ^2-values are listed in the summary Table 4.

5.3. Strontium adatom

As stated before, depending on the annealing conditions different kind of reconstructions have been found [12–15]. Most of the studies agree on the effect of ordering of oxygen vacancies at the surface. However, Kubo and Nozoye [17,16] argue that these reconstructions are formed by additional Sr atoms on the surface. The coverage and subsequent ordering of these adatoms, form a whole range of different reconstructions. In case of a (1×1) reconstructed surface, this means that there are two possibilities. Either the coverage of adatoms is zero, which is equivalent with a normal TiO_2-terminated crystal, or on top of the TiO_2 layer, a complete Sr layer exists. The latter is equivalent to having a SrO-terminated surface, and subsequently removing all the Oxygen. Here, we investigate the model in which the coverage of Sr-adatoms is one, because when the coverage is zero the structure resembles the one where rumpling occurs (Section 5.1). Kubo et al. reported relaxations for the topmost Sr layer and the two layers underneath, where in each layer both kind of atoms displace equally. To test this model we have used the displacements given by Kubo et al. and we have obtained displacements by fitting this model to our data. The resulting *R*-factors and χ^2-values are shown in summary Table 4.

5.4. Lateral displacement

Ravikumar et al. [41] suggested a model in which the top layer of the SrO-terminated surface displaces laterally. Both the Sr and O shift along the same principle axis, although with different magnitudes and in opposite directions. The TiO_2-terminated surface should not undergo such a reconstruction. In case of the mentioned lateral displacement, the planar P4mm symmetry would be broken. However, the results of merging (see Section 4) do not indicate the absence of mutually perpendicular mirror planes in the *ab*-plane. Therefore the validity of this model is tested under the assumption of four different co-existing domains, related through 90° rotation around the [0 0 1] direction. The results of using the findings of Ravikumar et al. and the present best fit results for SrO and TiO_2-terminated surfaces with lateral displacements are listed in Table 4.

5.5. Oxygen overlayer model

Already from a qualitative analysis of the shapes of the CTRs, calculated by using different literature models, it becomes clear that none of them reproduces the data very well. Those models where no *z*-displacements of the Sr and Ti atoms are used, such as the low temperature-like structure and the lateral displacement (Sections 5.2 and 5.4 respectively), give the best result. This would indicate that the crystal is bulk terminated. The shapes of the rods with high in-plane momentum transfer or having both *h* and *k* odd, are described quite accurately by the bulk terminated model. In contrast, the two dips at lower and higher momentum transfer of the 201 Bragg point, shown in Fig. 2, are not well described by assuming bulk termination. The CTRs having a different shape, as discussed in Section 2.2, also seem to have a different scale factor. This can be seen in Fig. 2 where the calculated bulk contributions for the 32 and 11 CTR seem to be too low in comparison with the experimental data. As stated before, this indicates that the heavier atoms, Sr and Ti, remain in their bulk positions. This leaves the oxygen to be considered as accounting for the differences seen between our data and a model using bulk termination. For the oxygen present in the structure there are in principle two different possibilities. First they could relax, either laterally or perpendicularly to the surface. However, in case of displacements of the oxygen, just like it is seen in Section 5.1, those alone do not give a satisfactory result for all CTRs. Second the occupancy of the oxygen could change. Assuming that subsequently to oxygen-outdiffusion of the topmost layer, ordering of the vacancies occurs, the occupancy change can be ruled out, since no fractional order peaks are found. Moreover, adjusting the occupancy of the oxygen does not solve the previously described problem of fitting all CTRs simultaneously. Therefore we propose a model in which the terminating layer consists of oxygen atoms on top of a TiO_2-terminated cell. These oxygen atoms occupy (x,y) positions: $(0,0)$, $(\frac{1}{2},0)$, $(0,\frac{1}{2})$ and $(\frac{1}{2},\frac{1}{2})$, thereby respecting the planar P4mm symmetry. Because the atomic scattering factor for these additional oxygen atoms falls off rapidly as function of $\frac{\sin(\theta)}{\lambda}$, they will contribute little to the higher order CTRs. The resulting CTRs are shown in Fig. 3 and the displacements are listed in Table 3. Fig. 4 shows the resulting structure.

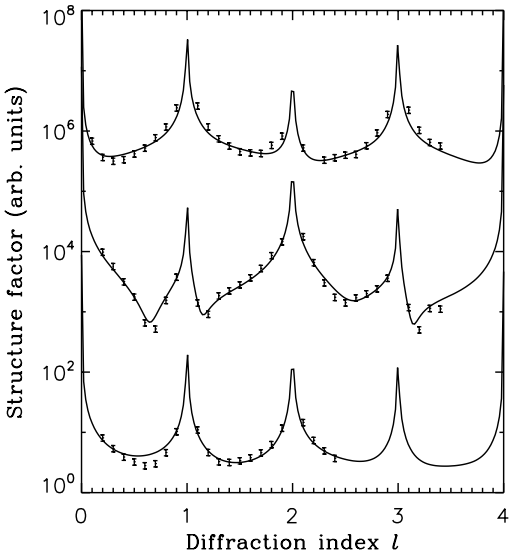

Fig. 3. Experimental data points and CTRs obtained with the oxygen overlayer model. Shown are the 32 (top), 20 (middle) and 11 (bottom) CTRs, where the error bars indicate the experimental data points.

Table 3
Refined positions and thermal parameters of the different atoms found for the present oxygen overlayer model. Fractional coordinates (x,y,z) are indicated, where z is zero in the bulk. Atom O4 is assumed to have an isotropic thermal parameter

Atom	x	y	z	$B_{\parallel}(\text{Å}^2)$	$B_{\perp}(\text{Å}^2)$
O1	0	0	1.08 ± 0.03	5 ± 4	10 ± 2
O2	$\frac{1}{2}$	0	1.037 ± 0.001	0.3 ± 0.7	0.4 ± 0.5
O3	$\frac{1}{2}$	$\frac{1}{2}$	1.04 ± 0.01	0.2 ± 0.7	3 ± 1
Ti	$\frac{1}{2}$	$\frac{1}{2}$	0.481 ± 0.005	1.0 ± 0.5	1.6 ± 0.5
O4	$\frac{1}{2}$	0	0.50 ± 0.01	0.7 ± 0.7	–

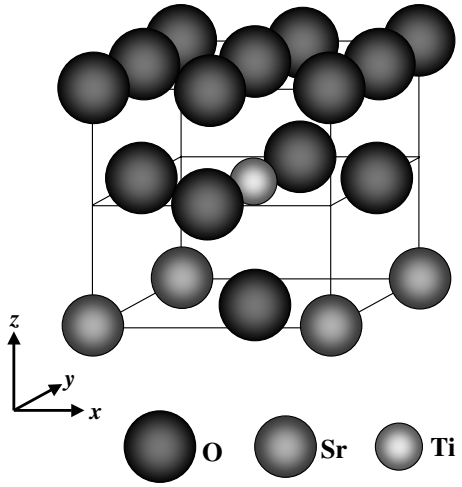

Fig. 4. Present model showing the oxygen overlayer on top of a TiO_2-terminated STO crystal. In the lowest SrO layer no relaxations are assumed, the displacements of the TiO_2 layer and oxygen overlayer are listed in Table 3.

The displacements listed in Table 3 are found with the data set of crystal 1. Using the data set of crystal 2 gives similar results, only the uncertainties in the thermal parameters are even larger. Another indication that the surfaces of the two crystals are well described by the oxygen overlayer model is seen in the overall scale factors obtained from the two fits. The ratio between the overall scale factors is exactly the scale factor that is applied when merging the two data sets (see Table 2). The resulting R-factors and χ^2-values are listed in Table 4.

The first questions that arise from the present model are where these additional oxygen atoms come from and what the bond lengths correspond to. It is well known that STO and similar compounds, like TiO_2, adsorb water [43], where usually the water oxygen (O_w) binds to the particular surface. In general, at temperatures lower than about 300 K water adsorbs as molecules, whereas at higher temperatures dissociation takes place and hydroxyl groups are formed [43]. The surface structure is also found to be of importance. In the case of rutile TiO_2, the (1 1 0) face adsorbs water molecularly in contrast to the (1 0 0) face, where dissociation of water takes place [44]. It is believed that depending on the distance of the O_w to the nearest binding site, one of the hydrogen detaches [44]. Recently, it was found that the TiO_2(0 1 1) (2×1) surface adsorbs water in a mixed molecular/dissociated state [45,46]. For TiO_2-terminated STO(0 0 1) it was found that defects, such as step edges and oxygen vacancies, act as catalytic centres for the dissociation of water [47,48]. Similar results with respect to defects on STO(0 0 1) were obtained for the adsorption and reaction of CO and CO_2 [49]. In the case of adsorption of water on the face of a crystal, one expects the water layer to be ordered due to the surface crystal structure. Water layers, completely in registry with the underlying crystal surface and partially disordered layers, have been found for several systems. In the case of KH_2PO_4 growth from the solution, Reedijk et al. [50] find water layers starting from completely ordered at the interface to completely disordered in the solution, with O–O distances of approximately 3 Å. The unstrained hydrogen bonded O–O distance is around 2.7 Å at room temperature. Similar water layers have been found on mica [51], whereas on hexagonal Ru(0 0 0 1) a ring-like structure resembling ice I_h and consisting of partially dissociated water [52], has been identified. In both systems the O–O distances are 2.5–2.7 Å, which suggests that they are hydrogen bonded. In the present model the shortest O–O bonds are close to 2 Å, which rules out normal hydrogen bonds. Even in ice X, known for its extremely short O–O distances, the pressure has to be well above 140 GPa in order to have the oxygen approach each other to about 2 Å [53]. On the other hand, Chu et al. [54] find an O–O distance of 2.3(1) Å for the electrochemical RuO_2(1 1 0)/water interface in an electric field of $\approx 10^9$ V/m,

Table 4
Overview of the resulting R-factors (Eq. (1)) and reduced χ^2[a] values for all different models as described in the text. Both SrO as well as TiO_2-terminated models are tested against the data of crystal 1 and crystal 2. Values for the R-factors are in %

Model	Crystal 1				Crystal 2			
	TiO_2		SrO		TiO_2		SrO	
	R	χ^2	R	χ^2	R	χ^2	R	χ^2
Surface rumpling								
Bickel et al.	47	20	61	26	62	30	73	36
Charlton et al.	37	14	52	21	49	21	64	29
Cheng et al.	47	19	54	23	59	26	64	29
Low temperature-like								
3° rotation	50	22	–	–	53	24	–	–
6° rotation	49	21	–	–	52	23	–	–
12° rotation	46	19	–	–	50	22	–	–
Lateral displacements								
Ravikumar et al.	–	–	52	17	–	–	57	21
Present	36	10	33	8.7	46	17	39	13
Sr adatom								
Kubo et al.	63	27	–	–	75	37	–	–
Present	29	8.3	–	–	38	12	–	–
Oxygen overlayer								
Present	16	2.3	–	–	26	5.8	–	–

[a] $\chi^2 = \frac{1}{N-p-1}\sum_{hkl}\frac{(|F_{obs}(hkl)|-s|F_{calc}(hkl)|)^2}{\sigma^2(F_{obs}(hkl))}$, with N the number of observed structure factors, p the number of refined parameters and s the overall scalefactor [42]. The errors, $\sigma(F_{obs})$, are mainly determined by the systematic errors, which have been taken twice the value R_{merge} of crystal 2 (see Section 4), resulting in 12%.

which obviously is the driving force for this particular O–O configuration. Reverting to the present model, it is arguable whether the O2 oxygens in the topmost layer are present. If absent, all O–O distances would be enlarged to approximately 2.8 Å, which would then suggest hydrogen bonding. The fit by leaving out the O2 oxygens in the topmost layer results in the underlying O4 oxygen to be pulled out of the Ti layer. However, the resulting χ^2 value becomes worse, and furthermore the particular features as described previously in the 20 and 22 CTRs are less well described. Another indication that O2 describes the experimental data rather well is seen in the temperature factors, shown in Table 3. These might even suggest that O1 is absent, which does not solve the problem of the short O–O distances. The possibility of adsorption of carbonates was examined as well (see [49]). For this the O2 was replaced by a carbon atom. Due to the similarity in atomic scattering factor between C and O, the fits are not substantially different, though with a slightly better χ^2 value for the oxygen overlayer model. However, the thermal parameters for the carbon become zero in the fit, and the subsequently refined occupancy becomes 1.25. Fitting the occupancy of O2 in the oxygen overlayer model, results in a value close to 0.9. Since the difference in atomic scattering factor, as used in ROD, between O and C is about 30% for small angles, the resulting occupancies and thermal parameters seem to indicate that indeed the atom at the $(\frac{1}{2},0)$ position should be oxygen. In the final oxygen overlayer model of which the results are listed in Table 3, no attempts were made at fitting the occupancies and all positions in the overlayer are assumed to be fully occupied. It seems that the O–O distances in the present model are too short to be hydrogen bonds and too long to be completely covalent bonds, like in molecular oxygen (1.2 Å), ozone (1.3 Å) or H_2O_2 (1.5 Å). The nature of the O–O bonds in the present model might be clarified by verifying the presence and/or location of hydorgen. Lopez et al. [55] find no signature of O–H bonds in their

Table 5
Preparation and experimental conditions for STO(001) surfaces by different authors

Author	Termination	Polishing/cleaning	Annealing	Experimental conditions
Charlton et al.	Double	Ar^+ sputtering	900 K, 10^{-6} mbar O_2	UHV
Bickel et al.	Double	Ar^+ sputtering	900 K, flash to 1400 K	UHV
Krainyukova et al.	Not reported	Chemo-mechanical	High temperature	UHV 170 K

high resolution electron energy loss spectroscopy (HREELS) study on clean STO(001) surfaces, unlike when Na is present. This might indicate that the surfaces used here are either not clean or that water dissociates completely into H_2 and O, like has been found for the Si(111)-7×7 surface [56]. Unfortunately, in the present study the used technique of SXRD is not sensitive to the scattering of hydrogen atoms. Furthermore, the current data do not include the specular CTR, which for very low angles would contain some information about hydrogen in the structure.

The fact that the literature models do not fit very well to our data might be attributed to the difference in characterization technique, experimental conditions or sample preparation, of which an overview is given in Table 5. All of the aforementioned authors have carried out their experiments in vacuum or presumed the crystals to be in vacuum for their calculations. Therefore, a similar experiment performed in vacuum and at elevated temperatures would allow for a more careful comparison. Next, the differences in sample preparation between the present work and the earlier studies result in different surfaces. The chemical treatment used here gives single terminated (001) surfaces, while other treatments result in double termination. However, all studies report (1×1) reconstructed surfaces. Finally, our experiment compares the best with the SXRD study of Charlton et al. Unfortunately, the data set that is obtained in that experiment is rather limited and not very sensitive to the oxygen in the surface. Furthermore, the fact that a double terminated crystal is used, complicates the matter even more, due to the increase in the number of fit parameters. Nevertheless, when assuming that there is indeed a layer covering the surface in air, which might very well disappear by Ar^+ sputtering, the structure of the TiO_2 layer underneath is differing only slightly from the bulk.

6. Conclusions

The atomic surface structure of single terminated $SrTiO_3$ (001) (1×1) crystals, obtained by chemical etching and annealing in oxygen, is studied in air using SXRD. AFM measurements confirm that the surface is single terminated and the absence of fractional order reflections in both RHEED and the present SXRD measurements indicate no lateral surface reconstruction. Two crystals, prepared in the same manner, are used in two different experiments. From the results of merging the two data sets it is concluded that both the preparation method as well as the SXRD experiments are carried out in a reliable and reproducible way. Models as proposed in literature cannot be fitted satisfactorily to our data. First of all, those models in which the heavier Ti and/or Sr atoms displace more than about 0.2 Å from their bulk positions, do not agree with the higher order SXRD data. Second, those models that keep the heavier atoms in their bulk positions, lack enough degrees of freedom for the oxygen to adequately fit the lower order data. A complete overview of the resulting *R*-factors (see Eq. (1)) and reduced χ^2 values for each of the model is given in Table 4. A model in which a TiO_2-terminated surface is completely covered by oxygen leads to the best fit. This oxygen overlayer model leads to O–O distances close to 2 Å. Since hydrogen bonds would result in O–O distances close to 2.7 Å, these short distances seem to rule out hydrogen bonding and would point towards a more covalent binding character between the nearest oxygen atoms. Most likely the oxygen overlayer is formed due to the (dissociative) adsorption of water, possibly occurring during the chemical etching or further surface treatment process. Verifying the presence of hydrogen would be very helpful in clarifying the nature of the oxygen overlayer, however the method used here is not capable of doing so. The

TiO_2 layer underneath the oxygen layer displays only slight rumpling, close to bulk termination. When comparing this with previous studies, this would be an indication that the surface is very stable, regardless UHV or preparation conditions.

Acknowledgements

The authors would like to thank the staff of ID03 and Dubble for help during the experiments, Dave Blank and Guus Rijnders for providing the samples and assistance with part of the data collection, Mark Huijben for the AFM measurements, Odile Robach for help with the program ROD and Elias Vlieg for critical reading of the manuscript. The Netherlands Organization for Scientific Research (NWO) is acknowledged for financial support.

References

[1] F. Jona, G. Shirane, Ferroelectric Crystals, Dover Publications, New York, 1993.
[2] G. Shirane, Y. Yamada, Phys. Rev. 177 (1969) 858.
[3] S.M. Shapiro, J.D. Axe, G. Shirane, Phys. Rev. B 6 (1972) 4332.
[4] K.A. Müller, W. Berlinger, Phys. Rev. Lett. 26 (1971) 13.
[5] R.A. Cowley, W.J.L. Buyers, G. Dolling, Solid State Commun. 7 (1969) 181.
[6] T. Sakudo, H. Unoki, Phys. Rev. Lett. 26 (1971) 851.
[7] W.G. Stirling, J. Phys. C: Solid State Phys. 5 (1972) 2711.
[8] G. Rijnders, S. Curràs, M. Huijben, D. Blank, H. Rogalla, Appl. Phys. Lett. 84 (2004) 1150.
[9] M. Kawasaki, K. Takahashi, T. Maeda, R. Tsuchiya, M. Shinohara, O. Ishiyama, T. Yonezawa, M. Yoshimoto, H. Koinuma, Science 266 (1994) 1540.
[10] M. Kawasaki, A. Ohtomo, T. Arkane, K. Takahashi, M. Yoshimoto, H. Koinuma, Appl. Surf. Sci. 107 (1996) 102.
[11] G. Koster, G. Rijnders, D.H.A. Blank, H. Rogalla, Physica C 339 (2000) 215.
[12] Q. Jiang, J. Zegenhagen, Surf. Sci. 367 (1996) L42.
[13] Q. Jiang, J. Zegenhagen, Surf. Sci. 425 (1999) 343.
[14] T. Nishimura, A. Ikeda, H. Namba, T. Morishita, Y. Kido, Surf. Sci. 421 (1999) 273.
[15] N. Erdman, L.D. Marks, Surf. Sci. 526 (2003) 107.
[16] T. Kubo, H. Nozoye, Surf. Sci. 542 (2003) 177.
[17] T. Kubo, H. Nozoye, Phys. Rev. Lett. 86 (2001) 1801.
[18] Y.A. Abramov, V.G. Tsirelson, V.E. Zavodnik, S.A. Ivanov, I.D. Brown, Acta Cryst. B 51 (1995) 942.
[19] I.K. RobinsonHandbook on Synchrotron Radiation, 3, North-Holland, Amsterdam, 1991 (Chapter 7) pp. 221–266.
[20] R. Feidenhans'l, Surf. Sci. Rep. 10 (1989) 105.
[21] G. Koster, B.L. Kropman, G. Rijnders, D.H.A. Blank, H. Rogalla, Mater. Sci. Eng. B 56 (1998) 209.
[22] G. Koster, B.L. Kropman, G. Rijnders, D.H.A. Blank, H. Rogalla, Appl. Phys. Lett. 73 (1998) 2920.
[23] S. Ferrer, F. Comin, Rev. Sci. Instrum. 66 (1995) 1674.
[24] M. Borsboom, W. Bras, I. Cerjak, D. Detollenaere, D.G. van Loon, P. Goedtkindt, M. Konijnenberg, P. Lassing, Y.K. Levine, B. Munneke, M. Oversluizen, R. van Tol, E. Vlieg, J. Synchr. Radiat. 5 (1998) 518.
[25] E. Vlieg, J. Appl. Cryst. 30 (1997) 532.
[26] E. Vlieg, J. Appl. Cryst. 31 (1998) 198.
[27] A. Munkholm, S. Brennan, J. Appl. Cryst. 32 (1999) 143.
[28] E. Vlieg, J. Appl. Cryst. 33 (2000) 401.
[29] J. Padilla, D. Vanderbilt, Surf. Sci. 418 (1998) 64.
[30] Z.Q. Li, J.L. Zhu, C.Q. Wu, Z. Tang, Y. Kawazoe, Phys. Rev. B 58 (1998) 8075.
[31] J. Prade, J. Phys.: Condens. Matter 5 (1993) 1.
[32] C. Cheng, K. Kunc, M.H. Lee, Phys. Rev. B 62 (2000) 10409.
[33] E. Heifets, R.I. Eglitis, E.A. Kotomin, J. Maier, G. Borstel, Phys. Rev. B 64 (2001) 235417.
[34] A. Ikeda, T. Nishimura, T. Morishita, Y. Kido, Surf. Sci. 433 (1999) 520.
[35] N. Bickel, G. Schmidt, K. Heinz, K. Müller, Phys. Rev. Lett. 62 (1989) 2009.
[36] T. Hikita, T. Hanada, M. Kudo, J. Vac. Sci. Technol. A 11 (1993) 2649.
[37] G. Charlton, S. Brennan, C.A. Muryn, R. McGrath, D. Norman, T.S. Turner, G. Thornton, Surf. Sci. 457 (2000) L376.
[38] E.D. Mishina, N.E. Sherstuyk, V.V. Lemanov, A.I. Morozov, A.S. Sigov, T. Rasing, Phys. Rev. Lett. 85 (2000) 3664.
[39] N.V. Krainyukova, V.V. Butskii, Surf. Sci. 454 (2000) 628.
[40] D.E. Sands, Vectors and Tensors in Crystallography, Addison-Wesley, New York, 1982.
[41] V. Ravikumar, D. Wolf, V.P. Dravid, Phys. Rev. Lett. 74 (1995) 960.
[42] P.R. Bevington, Data Reduction and Error Analysis for the Physical Sciences, McGraw-Hill, New York, 1969.
[43] P. Thiel, T.E. Madey, Surf. Sci. Rep. 7 (1987) 211.
[44] M.A. Henderson, Langmuir 12 (1996) 5093.
[45] T.J. Beck, A. Klust, M. Batzill, U. Diebold, C. DiValentin, A. Tilocca, A. Selloni, Surf. Sci. Lett., in press.
[46] C. DiValentin, A. Tilocca, A. Selloni, T.J. Beck, A. Klust, M. Batzill, Y. Losovvj, U. Diebold, J. Am. Chem. Soc. 127 (2005) 9895.
[47] R.G. Egdell, P.D. Naylor, Chem. Phys. Lett. 91 (1982) 200.
[48] N.B. Brookes, G. Thornton, F.M. Quinn, Solid State Commun. 64 (1987) 383.
[49] S. Azad, M.H. Engelhard, L.-Q. Wang, J. Phys. Chem. B 109 (2005) 10327.
[50] M.F. Reedijk, J. Arsic, F.F.A. Hollander, S.A. de Vries, E. Vlieg, Phys. Rev. Lett. 90 (2003) 066103.
[51] L. Cheng, P. Fenter, K.L. Nagy, M.L. Schlegel, N.C. Sturchio, Phys. Rev. Lett. 87 (2001) 156103.

[52] J. Weissenrieder, A. Mikkelsen, J.N. Andersen, P.J. Feibelman, G. Held, Phys. Rev. Lett. 93 (2004) 196102.
[53] M. Benoit, D. Marx, M. Parrinello, Nature 392 (1998) 258.
[54] Y.S. Chu, T.E. Lister, W.G. Cullen, H. You, Z. Nagy, Phys. Rev. Lett. 86 (2001) 3364.
[55] A. Lopez, T. Heller, T. Bitzer, Q. Chen, N. Richardson, Surf. Sci 494 (2001) L811.
[56] R.-L. Lo, I.-S. Hwang, T. Tsong, Surf. Sci 530 (2003) L302.